Available online at www.sciencedirect.com

ScienceDirect

IFAC PapersOnline CONFERENCE PAPER ARCHIVE

IFAC PapersOnLine 52-14 (2019) 213–218

Computational cost of an exergy-based fault detection scheme implemented in a commercial process simulator

Henri Marais * **George van Schoor** ** **Kennith R. Uren** ***

* *School of Electrical, Electronic, and Computer Engineering, North-West University, Potchefstroom, South Africa, 2531 (email: henri.marais@nwu.ac.za)*

** *Unit for Technology and Energy Systems, North-West University, Potchefstroom, South Africa, 2531 (email: george.vanschoor@nwu.ac.za)*

*** *School of Electrical, Electronic, and Computer Engineering, North-West University, Potchefstroom, South Africa, 2531 (email: kenny.uren@nwu.ac.za)*

Abstract: Energy-based fault detection and isolation (FDI) schemes show promise in terms of applicability to petrochemical industries and the broader process industries. Model-based FDI schemes offer pronounced advantages over more easily implemented data-driven FDI techniques. However, the implementation of model-based FDI schemes require the development of analytic models, and as such, widespread adoption is lacking. Although process simulators derive analytic models internally, comprehensive exergy-based parameters are not calculated automatically. In this work Aspen Hysys is extended by means of user variables to allow the automatic calculation of physical and chemical exergy for each process stream. Initial results indicate that additional computational overhead of approximately 20% is incurred and that the calculation technique scales well with model size. This calculation method allows the development of a truly hybrid model- and data-based approach to FDI within the process industries.

Keywords: Process, Simulation, Fault, Identification, Automatic

1. INTRODUCTION

The rise of the Internet of Things (IoT) can be seen as one enabling element of the fourth industrial revolution (Industry 4.0). Amongst others, one of the advantages of Industry 4.0 is that process efficiency and maintenance processes can be improved significantly. These advantages are premised on the ability to accurately and cost-effectively measure operational parameters of processes, machines, and systems and predict if or when failures will occur. For the petrochemical industries (PCI) these advantages are significant. However, to date, the achievable advantages fall short, mainly due to the complexity of performing fault detection.

In Section 2 a review of current fault detection and isolation techniques is presented with an alternative approach to FDI being proposed in Section 3. A suitable case-study is developed in Section 4 from which the automatic calculation of key parameters can be developed in Section 5. Initial results and concluding remarks are provided in Section 6.

2. FAULT DETECTION AND IDENTIFICATION

As a field of study, fault detection and isolation (FDI) can be seen as a subset of fault detection and diagnosis (FDD). The latter being concerned with quantification of the severity of identified faults or malfunctions in a system. However, due to similarities in the identification and localisation taks between FDD and FDI, FDI seems the more commonly used term. Semantically FDI and condition monitoring is closely related and as such only FDI is considered in this work.

With regards to the PCIs specifically, the study of FDI techniques has seen a near two fold increase since 2010 according to Ming and Zhao (2017). FDI approaches are classified as either model-based (requiring analytical models) or data-driven (relying solely on historic process data) as outlined by Venkatasubramanian (2001).

However, perusal of the PCI FDI literature indicates that most authors apply statistical techniques such as PCA (Jiang et al. (2017)), PLS (Sheriff et al. (2017)) and the non-linear variations of these techniques (Qin (2009)). According to Ghosh et al. (2014), the lack of model-based schemes are typically attributed to the extensive relaince on expert knowledge (limited and expensive) and the sheer complexity of developing analytical models of PC plants. FDI techniques are typically applied to simulated benchmark processes such as the Tennessee Eastman process (Yin et al. (2012) and Ammiche et al. (2018)) which is not surprising when considering that a single process unit could have up to 1000 monitored variables according to Ming and Zhao (2017). Additionally, it has

2405-8963
Peer review under responsibility of International Federation of Automatic Control.
10.1016/j.ifacol.2019.09.189

been shown that excessive inclusion of process variables could not only increase the computational complexity and the dimensionality of the process but degrade the FDI scheme's performance (Ghosh et al. (2014)).

From the work of Venkatasubramanian et al. (2003), it is unlikely that a single FDI scheme would provide acceptable performance across a range of operational environments. This has lead to the development of hybrid FDI schemes where multiple techniques are combined. In the work of Mallick and Imtiaz (2013) a combination of PCA and a Bayesian Belief Network (BNN) was applied to a dissolution tank. Martins et al. (2015) applied a combination of statistical and machine learning techniques to a coupled two-tank system and Qin (2009) applied a combination of statistical techniques to a polymer film process. Commonly, hybrid FDI takes the form of a signal-based part (statistical techniques such as PCA dominate) followed by a data-based part (where artificial neural networks (ANNs) dominate) according to Cecati (2015). From the perspective of the authors this approach is purely a combination of data-driven approaches and not a true hybrid model- and data-based scheme.

3. HYBRID FDI

From the preceding section, the lack of model-based FDI schemes in the PCIs can be attributed to the modelling complexity that these schemes pose. However, model-based FDI techniques offer the advantage of not requiring a labeled (and uaually large) historic process data set. For this reason, methods of implementing model-based FDI in PCI (or other process industries) needs to be investigated. The reduction of model order has received significant attention with several techniques being quite common (Elrazaz and Sinha (1981)). Of the available techniques significant effort has been devoted towards linear, non-parametric processes and the application of these metods to numerical simulation acoording to Benner et al. (2015). However, a wide-spread technique used in engineering is the simplification of the underlying physics or the transformation from one problem domain to another. These transformations, eg. time-domain to frequency-domain, is common in signal processing and control theory literature.

3.1 Energy-based FDI

By representing all of the system interactions in the energy domain the modelling space is essentially *flattened* to a single domain. The use of energy as a modelling domain for industrial-scale systems is not new (Chinneck and Chandrashekar (1984)). However, perusal of energy-based FDI literature indicates that the *energy* referred to is usually with reference to energy components in the frequency spectral domain (Derek Li (2017)) or energy of wavelet features (Jung and Koh (2015)). However, Fouché et al. (2016) showed that fault detection and isolation of an axial-flow compressor could be accomplished by means of studying physical energy flows and Uren and van Schoor (2016) accomplished similar results for a heat exchanger. From a thermodynamic perspective, cycle operation can be represented on an entropy-ehtnalpy ($h-s$) graph. In the work of du Rand and van Schoor (2012) an energy-based

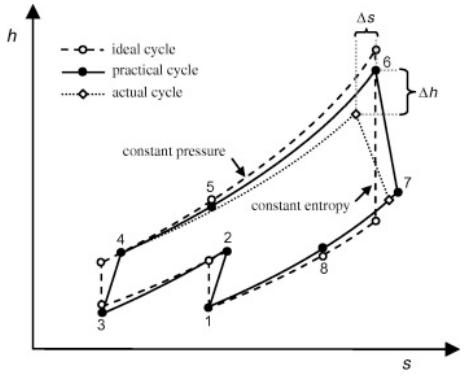

Fig. 1. Representative sample of the Du Rand energy-signature

technique was used to monitor the health of a Brayton-cycle nuclear power plant by making use of an ($h-s$) graph such as that in Figure 1.

Ming and Zhao (2017) asserts that FDI schemes are typically unavailable during process transitions (start-up and shut-down especially), however, the technique proposed by du Rand and van Schoor (2012) can be utilised, without modification, to various operating points which is a significant advantage of the model-based energy-based FDI scheme above data-driven approaches.

3.2 Exergy-based FDI

However, as shown by Marais et al. (2016) the transformation to a single energy domain has limits when applied to processes where chemical transformation takes place. When only considering the energy-domain, perfect fault detection could be achieved but perfect isolation was impossible. Thus, an alternative to the energy-domain needs to be used. Exergy is defined as the fraction of energy contained in a system that can be used to perform work (Sciubba and Wall (2007)).

It is common that PC plants are heavily affected by environmental paramenters such as temperature and that this is difficult to accurately model. Zaleta-Aguilar et al. (2018) showed that exergy-based characterisation could be used to determine the *normal* operating range of a gassifier given environmental variations. Essentially the exergetic efficiency of each process unit is determined by considering all exergy inflows, outflows, losses, and heat generation. A simple comparison between the expected and measured efficiency parameters would thus be indicative of a malfunction. The detection of a possible malfunction is accomplished by comparing the actual β (total extensive exergy) value at A, against the expected value at a reference point R. Any deviation would be indicative of a malfunction (as indicated in Figure 2). It should be noted that the technique proposed by Zaleta-Aguilar allows for the variation in system performance due to environmental changes to be accurately captured.

Thermo-characterisation can be mathematically intensive (as evidenced by the work of Zaleta-Aguilar et al. (2018)) and the use of exergy as an FDI scheme could therefor be limited; especially for systems with many distinct process units. However, Marais et al. (2017) has successfully used a process simulator (Aspen HySys) to perform exergy-based

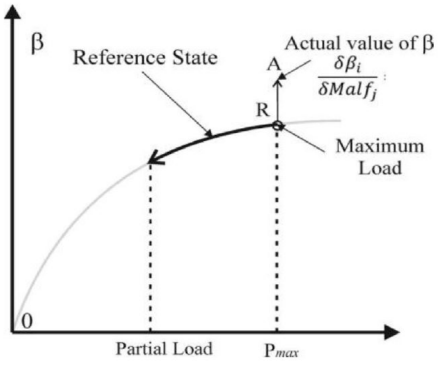

Fig. 2. Effect of maulfunction of β at a specific load (from Zaleta-Aguilar et al. (2018))

FDI for an auto-thermal reformer (ATR) and in Greyling S (2019) the application of an exergy-based FDI scheme to a GTL process plant is detailed.

3.3 Exergy calculation

According to de Oliveira Junior (2012) the maximum work expendable by a substance entering a control volume is defined as

$$b = [h_i - h_0 - T_0(s_i - s_0)], \tag{1}$$

where b is referred to as the exergy, and h, s, and T refer to the associated enthalpy, entropy, and temperature. The subscripts i and 0 denote the current and reference environment respectively. However, total exergy is an algebraic sum of several domain specific exergies, such that:

$$b_{tot} = b_{kin} + b_{pot} + b_{ph} + b_{ch}, \tag{2}$$

where b_{kin} and b_{pot} refer to the kinetic and potential exergy of the system, and b_{ph} and b_{ch} to the physical and chemical exergy respectively. However, when considering a typical process plant, during normal operations the plant is unlikely to move, and as such, the kinetic and potential exergy of the plant itself can be ignored. As for the kinetic and potential energy of the material steam, that have already been accounted for in the physical exergy associated with the stream. Subsequently (2) simplifies to:

$$b_{tot} = b_{ph} + b_{ch}. \tag{3}$$

The physical exergy associated with a substance is simply a function of its thermodynamic state. Formally, physical exergy $b_{ph}$is defined as the energy that would be required to take the substance from its current thermodynamic state (T, p), to that of the standard reference environment (SRE) which is typically defined as existing at a T_0 of 25 °C and a pressure p_0 of 1 atm. Subsequently,

$$b_{ph} = (h - h_0) - T_0(s - s_0), \tag{4}$$

It is clear that there is a strong similarity between the physical exergy b_{ph} and the work of du Rand and van Schoor (2012). The chemical exergy of any chemical compound n can be calculated by:

$$b_{ch\,n} = \Delta G_f + \sum_e n_e b_{ch\,e} \tag{5}$$

in which, ΔG_f is the heat of formation, n_e the amount of substance n and $b_{ch\,e}$ chemical exergy of substance n.

Chemical exergy is defined as the energy available to do work when the substance undergoes a reversible process from the restricted reference state (25 °C, 1 atm) to a thermodynamically dead state in which the system is in complete thermodynamic equilibrium (thermal, pressure, and chemical) (de Oliveira Junior (2012)). Conceptually, then, chemical exergy quantifies the value of a chemical substance, or compound, as measured against a selected reference environment.

For the purposes of exergy calculation the definition of the standard reference environment (SRE) is a point of contention, especially insofar as chemical exergy is concerned. The SREs of Szargut Szargut et al. (2005) and Ahrendts dominate but the SRE proposed by Szargut seems to be more commonly used in engineering systems Sciubba and Wall (2007) and is thus used in this work.

In Szargut et al. (2005) a detailed breakdown is provided on how each of the reference elements is selected and henceforth, how the chemical exergy is calculated for each element. A typical implementation of Szargut's SRE may contain as many as 49 reference elements (Rivero and Garfias (2006)), and must consist of elements from the atmosphere, hydrosphere, and lithosphere.

In Szargut et al. (2005) the chemical exergy as well as the energy of formation are provided for all of the reference elements considered. A reference table provided by Szargut (2007) contains the exergy values of all SRE elements in addition to several common chemical compounds (that don't form part of the SRE). From a computational perspective then, it makes more sense to use a reference table rather than continually calculating the chemical exergy from the reference elements.

In the work of Zaleta-Aguilar et al. (2018) chemical exergy was calculated form first principles using the Gibbs free-energy model. Abdollahi-Demneh et al. (2011) proposed using an extension functionality in Aspen Hysys but made use of a non-standard reference environment and also required the exergy calculations to be performed from first principles for each component in the system at each simulation step; An approach which is computationally inefficient. However, since Aspen Hysys already incorporates the Gibbs free-energy model as standard in addition to incorporating the energy of mixing, extending Aspen Hysys in a computationally efficient manner could allow more widespread adoption of exergy-based FDI schemes.

4. PROCESS MODELLING OF AN AUTOTHERMAL REFORMER

In a gas-to-liquids (GTL) process, feedstock (typically methane gas) is reformed into syngas that is used to develop transportation fuels, parafins, and waxes (de Klerk (2012)). Of the various process units the reformer is typically the most costly from both a capital and operational perspective. It therefor follows, that any process improvements would, ideally, be made to the reformer. In Figure 3, a schematic representation of an autothermal reformer (ATR) is provided. In essence the ATR reforms a hydrocarbon-rich feedstock (such as methane) into a

more usable product by means of partial combustion in a controlled environment.

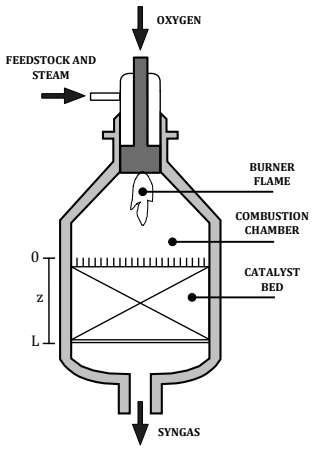

Fig. 3. Schematic representation of an autothermal reformer from Marais et al. (2016)

Aspen Hysys is a commercially available process simulator hys (2009) in which an ATR plant can be simulated. In Figure 4 the Aspen Hysys model of the ATR is shown. Note that the oxygen (O2) and carbondioxide (CO2) streams are automatically controlled by the simulation to reach the desired steady state set-points.

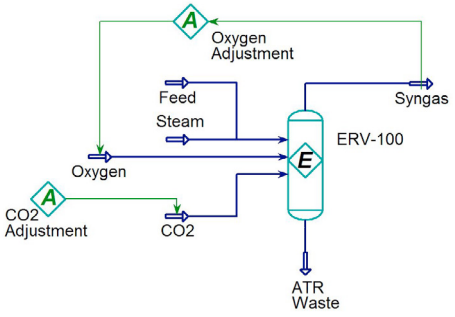

Fig. 4. Hysys process model of an ATR from Marais et al. (2017)

5. AUTOMATIC EXERGY CALCULATION

In order to implement the exergy-based FDI scheme as proposed by Marais et al. (2016) the physical and chemical exergy of each of the process stream in Figure 4 needs to be calculated. Aspen Hysys calculates the physical exergy of process streams automatically, however, no mechanism is provided to calculate chemical exergy. It is suspected that the primary argument against doing so is the complexity involved in supporting multiple SREs together with the computation overhead incurred. However, for the purposes of exergy-based FDI automatic calculation is required.

By making use of a mechanism referred to as *User Variables* within the Hysys environment the user can extend the functionality of the simulator by means of Visual Basic for Applications (VBA) procedures. In Algorithms 1 and 2 pseudo code is presented to accomplish the calculation of both physical and chemical exergy.

5.1 Physical Exergy

By inspection, Algorithm 1 implements (4). Aspen Hysys groups parameters related to a specific stream together into a *Stream* object of which the constituent properties can be accessed by means of the standard object-oriented dot notation. Line 7 in Algorithm 1 forces a recalculation of the current stream's entropy and enthalpy values for the provided reference environment by means of an Aspen Hysys command `TPFlash()`. It should be noted that the use of Algorithm 1 is preferred to the integrated functionality as it allows the explicit definition of the SRE's temperature and pressure.

Algorithm 1. Calculation of physical exergy (B_{ph})

Require: Reference environment temperature T_{ref} and pressure P_{ref} in simulation basis

1: $Stream \leftarrow Stream_{Simulated}$
2: **if** `Stream.VapourFractions.IsKnown` **and** `Stream.MolarFractions.IsKnown` **and** `Stream.MolarFlow.IsKnown` **then**
3: $H \leftarrow Stream.Enthalpy$
4: $S \leftarrow Stream.Entropy$
5: $Stream.Temperature \leftarrow T_{ref}$
6: $Stream.Pressure \leftarrow P_{ref}$
7: $Stream.TPFlash()$
8: $H_0 \leftarrow Stream.Enthalpy$
9: $S_0 \leftarrow Stream.Entropy$
10: $B_{ph} \leftarrow (H - H_0) - (T_{ref} + 273.15)(S - S_0)$
11: $F \leftarrow$ `Stream.MolarFlow.GetValue("kgmole/h")`
12: $B_{ph} \leftarrow B_{ph}F$
13: **end if**

5.2 Chemical Exergy

The chemical exergy associated with a component can be calculated by means of a tedious process. However, regardless of the generation mechanism involved, the chemical exergy of the component remains fixed (relative to the SRE). As such, making use of reference tables is a computationally efficient solution which simplifies (5) to

$$b_{ch\ total} = \sum_{comp} n_{comp} b_{ch\ comp}. \tag{6}$$

In essence requiring only the table of reference exergies per component ($b_{ch\ comp}$) of interest and the fraction of said component in mixture (n_{comp}). Algorithm 2 is used to calculate the chemical exergy of an associated simulation stream based on (6). Note that Line 7 in Algorithm 2 is used to request the chemical exergy of the specific component from the simulation basis. If this value has not been defined the resulting calculation will under report the stream's total chemical exergy. This also allows to experiment with the component(s) of interest in a stream as opposed to using all stream components.

6. RESULTS AND CONCLUSION

Installation of user-variables based on Algorithm 1 and 2 affects all material and energy streams. As such, the additional computation overhead (expressed as an increase in simulation time) needs to be investigated.

Algorithm 2. Calculation of chemical exergy (B_{ch})

Require: Components' chemical exergies defined in simulation basis

$Stream \leftarrow Stream_{Simulated}$
if (`Stream.VapourFractionValue` = 1) **and** `Stream.MolarFlow.IsKnown` **and** `Stream.MolarFractions.IsKnown` **then**
  $B_{ch} \leftarrow 0$
  $i \leftarrow 0$
  for $i < Stream.Components.Count - 1$ **do**
    Comp = Stream.Components.Item(i)
    $B_{ch_{comp}} \leftarrow$ `Comp.GetUserProperty("Bch")`
    $C_{frac} \leftarrow$ `Stream.MolarFractionsValue(i)`
    $B_{ch} \leftarrow B_{ch} + B_{ch_{comp}}.C_{frac}$
  end for
  $F \leftarrow$ `Stream.MolarFlow.GetValue("kgmole/h")`
  $B_{ch} \leftarrow B_{ch}F$
end if

In Table 1 summary data of 5 successive simulation runs of the ATR are provided. Although there is a clear increase of about 21% in the overall simulation run time, the total run time of approximately one second is quite short. As such, these results may not be indicative of larger process simulations.

Table 1. Effect of user-variable inclusion on ATR simulation time

	Default (s)	User-Vars. (s)	Change (%)
Run 1	0.95	1.20	+26.32
Run 2	0.99	1.17	+18.18
Run 3	1.30	1.49	+14.62
Run 4	0.98	1.22	+24.49
Run 5	1.19	1.45	+21.85
Average	1.08	1.31	+20.70
Mean	0.99	1.22	+23.23
Std Dev.	0.138	0.135	-1.99

To investigate the effect of simulation scale a similar experiment was conducted on a complete GTL process simulation consisting of 12 process units (including an ATR) and 25 process streams.

The Aspen Hysys process flow diagram of the GTL plant as shown in Figure 5 is provided out of interest's sake as the details of the development is outside the scope of this article. In Table 2 the results of the GTL simulation is provided.

Table 2. Effect of user-variable inclusion on GTL process simulation time

	Default (s)	User-Vars. (s)	Change (%)
Run 1	7.64	9.55	+25.00
Run 2	7.40	10.75	+45.27
Run 3	8.17	9.7	+18.73
Run 4	18.24	20.46	+12.17
Run 5	7.80	9.25	+18.59
Run 6	7.73	9.23	+19.4
Average	9.50	11.49	+23.19
Median	7.77	9.63	+19.07
Std Dev.	3.92	4.04	+10.55

It is interesting to note from Table 2 that the additional simulation time incurred due to the inclusion of the user variables are comparable to those of the smaller ATR

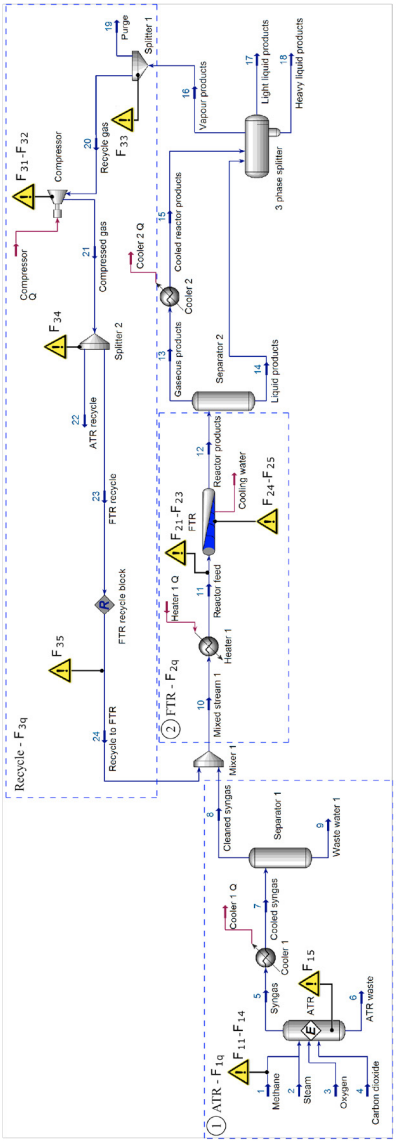

Fig. 5. Process flow diagram of a GTL process

process even though the GTL simulation is an order of magnitude more complex from a process unit perspective.

The exact reason for the variance between successive simulation runs in Tables 1 and 2 is unknown but underlying optimisation algorithms might be the root cause for this. However, a comparison between the descriptive statistics show that the inclusion of the automatic exergy calculation is not overly expensive from a simulation run-time perspective. Exclusion of the apparent outlier (Run 4 in 2) reduces the standard deviation when using user variables to 0.56, however, the effect on the % difference descriptive statistics is negligible.

It should be kept in mind that a process simulator (such as Aspen Hysys) essentially constructs an analytical model (albeit simplified, or otherwise subject to model reduction techniques) of the target process. As such, the implementation of the automatic exergy calculation allows the implementation of model-based FDI schemes to simulated processes. Energy-based (and per extension exergy-based)

FDI schemes show promise in terms of process transient behaviour. The additional computation time incurred can easily be offset by the reduced modelling effort required due to the use of a process simulator and would allow the development of truly hybrid FDI techniques.

REFERENCES

(2009). *AspenONEV7. 0 Documentation*. AspenTechnology, Inc., Burlington, Massachusetts, v7.0 edition.

Abdollahi-Demneh, F., Moosavian, M.A., Omidkhah, M.R., and Bahmanyar, H. (2011). Calculating exergy in flowsheeting simulators: A hysys implementation. *Energy*, 36(8), 5320–5327.

Ammiche, M., Kouadri, A., and Bakdi, A. (2018). A combined monitoring scheme with fuzzy logic filter for plant-wide tennessee eastman process fault detection. *Chemical Engineering Science*, 187, 269 – 279.

Benner, P., Gugercin, S., and Willcox, K. (2015). A survey of projection-based model reduction methods for parametric dynamical systems. *SIAM Review*, 57, 483–531.

Cecati, C. (2015). A survey of fault diagnosis and fault-tolerant techniques—part ii: Fault diagnosis with knowledge-based and hybrid/active approaches. *IEEE Transactions on Industrial Electronics*.

Chinneck, J. and Chandrashekar, M. (1984). Models of large-scale industrial energy systems—i. simulation. *Energy*, 9(1), 21–34.

de Klerk, A. (2012). *Fischer-Tropsch Refining*. John Wiley & Sons.

de Oliveira Junior, S. (2012). *Exergy: production, cost and renewability*. Springer Science & Business Media.

Derek Li, D.W. (2017). An energy spectral technique for induction motor fault detection. *2017 International Conference on Sensing, Diagnostics, Prognostics, and Control (SDPC), 2017 International Conference on, SDPC*, 704.

du Rand, C. and van Schoor, G. (2012). Fault diagnosis of generation iv nuclear htgr components – part i: The error enthalpy–entropy graph approach. *Annals of Nuclear Energy*, 40(1), 14 – 24. doi: https://doi.org/10.1016/j.anucene.2011.09.013.

Elrazaz, Z. and Sinha, N.K. (1981). A review of some model reduction techniques. *Canadian Electrical Engineering Journal*, 6(1), 34–40.

Fouché, L., Uren, K., and van Schoor, G. (2016). Energy-based visualisation of an axial-flow compressor system for the purposes of fault detection and diagnosis. *IFAC-PapersOnLine*, 49(7), 314–319.

Ghosh, K., Ramteke, M., and Srinivasan, R. (2014). Optimal variable selection for effective statistical process monitoring. *Computers & Chemical Engineering*, 60, 260–276.

Greyling, S., Marais, H., Van Schoor, G., Uren, K.R. (2019). Application of exergy-based fault detection in a gas-to-liquids process plant. *entropy*, 21(6: 565).

Jiang, X., Zhao, H., and Leung, H. (2017). Fault detection and diagnosis in chemical processes using sparse principal component selection. *Journal of Chemical Engineering of Japan*, 50(1), 31–44.

Jung, Uk1, u. and Koh, B.H. (2015). Wavelet energy-based visualization and classification of high-dimensional signal for bearing fault detection. *Knowledge & Information Systems*, 44(1), 197 – 215.

Mallick, M.R. and Imtiaz, S.A. (2013). A hybrid method for process fault detection and diagnosis. *IFAC Proceedings Volumes*, 46(32), 827–832.

Marais, H., van Schoor, G., and Uren, K.R. (2017). The merits of exergy-based fault detection in petrochemical processes. *Journal of Process Control*.

Marais, H.J., van Schoor, G., and Uren, K.R. (2016). Energy-based fault detection for an autothermal reformer. *IFAC-PapersOnLine*, 49(7), 353–358.

Martins, R.S., Vale, M.R., and Maitelli, A.L. (2015). Hybrid methods for detection and identification of faults in dynamic systems. *Asian Journal of Control*, 17(5), 1831–1847.

Ming, L. and Zhao, J. (2017). Review on chemical process fault detection and diagnosis. In *Advanced Control of Industrial Processes (AdCONIP), 2017 6th International Symposium on*, 457–462. IEEE.

Qin, S.J. (2009). Data-driven fault detection and diagnosis for complex industrial processes. *IFAC Proceedings Volumes*, 42(8), 1115 – 1125. 7th IFAC Symposium on Fault Detection, Supervision and Safety of Technical Processes.

Rivero, R. and Garfias, M. (2006). Standard chemical exergy of elements updated. *Energy*, 31(15), 3310–3326.

Sciubba, E. and Wall, G. (2007). A brief commented history of exergy from the beginnings to 2004. *International Journal of Thermodynamics*, 10(1), 1–26.

Sheriff, M.Z., Botre, C., Mansouri, M., Nounou, H., Nounou, M., and Karim, M.N. (2017). Process monitoring using data-based fault detection techniques: Comparative studies. In *Fault Diagnosis and Detection*. InTech.

Szargut, J. (2007). *Egzergia. Poradnik obliczania I stosowania*. Widawnictwo Politechniki Shlaskej.

Szargut, J., Valero, A., Stanek, W., and Valero, A. (2005). Towards an international legal reference environment. *Proceedings of ECOS*, 2005, 409–20.

Uren, K.R. and van Schoor, G. (2016). Energy-based visualisation of a counter-flow heat exchanger for the purpose of fault identification. *IFAC-PapersOnLine*, 49(7), 19–24.

Venkatasubramanian, V. (2001). Process fault detection and diagnosis: past, present and future. *IFAC Proceedings Volumes*, 34(27), 1–13.

Venkatasubramanian, V., Rengaswamy, R., Yin, K., and Kavuri, S.N. (2003). A review of process fault detection and diagnosis: Part i: Quantitative model-based methods. *Computers & Chemical engineering*, 27(3), 293–311.

Yin, S., Ding, S.X., Haghani, A., Hao, H., and Zhang, P. (2012). A comparison study of basic data-driven fault diagnosis and process monitoring methods on the benchmark tennessee eastman process. *Journal of Process Control*, 22(9), 1567 – 1581.

Zaleta-Aguilar, A., Rodriguez-Alejandro, D., and Rangel-Hernández, V. (2018). Application of an exergy-based thermo characterization approach to diagnose the operation of a biomass-fueled gasifier. *Biomass and Bioenergy*, 116, 1–7.